Assessment of Landslide Recurrence by Onsite Monitoring - Incidence of Hong-yeh Landslide -

Chia-Chun WU[1,*], Pei-Hsi WANG[2], Chih-Hui WANG[3], Ching-Yen CHANG[3] and Te-Ling WU[3]

[1] Dept. of Soil and Water Conservation, National Pingtung University of Science and Technology (Neipu, Pingtung 92101, Taiwan)

[2] Lipang Engineering Consultant Co. Ltd. (Kaohsiung 80755, Taiwan)

[3] Taitung Branch, Soil and Water Conservation Bureau, Council of Agriculture, Executive Yuan (Taitung 95055, Taiwan)

*Corresponding author. E-mail: ccwu@mail.npust.edu.tw

Typhoon Meranti invaded Taiwan from Sept. 12 through 16 in 2016 and brought 633 mm of rain in 48 hours. A large-scale landslide behind Hong-Yeh Village of Taitung County consequently occurred on Sept. 15, which produced 40,000 m^3 of debris. Debris that affecting local settlement and blocking the bridge clearance was dredged. Countermeasure structures were immediately designed and implemented. Locations for permanent resettlement were evaluated. Nevertheless, uncertainty of landslide recurrence and feasibility of the countermeasures in coping with future disaster either caused by landslide or debris flow has troubled the government agencies. Hence, field geological survey, outcrop assessment, micro-terrain interpretation, core samples from core drills, Electrical Resistivity Image Profiling, and inclination as well as water stage readings from five boreholes were used to assess the likelihood of landslide recurrence. All evidence gathered onsite suggested the recurrence of landslide is highly possible. The unstable mass situated on upper landslide site displaced another 6.5 m eastward along the slope after a 5-day 924-mm torrential storm with peak one-day rainfall of 407 mm. Numerical simulations at different storm return periods with countermeasure designs scenarios were conducted to ensure the safety of Hong-Yeh Village and the functionality of countermeasure structures from debris-flow disaster. Adjustments on structure design were made accordingly and were implemented onsite, which helped reduce the areas of risk scope by 40.1%.

Key words: landslide, recurrence assessment, onsite monitoring, numerical simulation

1. INTRODUCTION

Typhoon Meranti invaded Taiwan from Sept. 12 through Sept. 16, 2016 and brought 633 mm of rain in 48 hours. A large-scale landslide occurred behind Hong-Yeh Village in Taitung County on Sept. 15, with an extent covering 7.8 ha from which 40,000 m^3 of debris were yielded. The front lobe of debris rushing downstream damaged 39 housings, three public buildings as well as local traffic system that situated at the foothill of the mountain range (**Fig. 1**).

A magnitude 5 earthquake trembled the entire Taitung County on Oct. 6, 2016 followed by Typhoon Aere that brought 1,010 mm of rain within a week. Earthquake and intensive rainfall further deteriorated the landslide and resulted a 1.8-ha expansion on landside scarp. Residents of Hong-Yeh Village were immediately evacuated.

Emergency relief task forces were immediately dispatched to help restore public facilities. Research team was also called up by government officials to conduct borehole drilling, to install monitoring system with the aim of assessing the recurrence of succeeding landslide, and to observe the possible movement of landslide scarp as well as changes of groundwater levels respectively.

Check dam and gully control structures were immediately designed and commissioned for construction. Debris that affecting local settlement was removed, and that blocking the clearance of bridge and torrent was dredged. Locations for permanent resettlement were evaluated.

Fig. 1 Disaster caused by September 15, 2016 landslide

Prior to landslide disaster, the torrent coded as DF-166 running through the Village has been announced as a debris-flow torrent with high recurrence potential. Eocene or earlier Hong-Yeh Stratum consisting of black slate with occasional inclusions of metamorphic sandstone covers most of the upper watershed; whereas gravel - sand - silt - clay terraced deposits from Late Pleistocene - Holocene period forms the geologic formation at the mid-lower watershed where Hong-Yeh Village was located. Fragile geology has brought about tension cracks as well as nonuniform slumps except large-scale landslide on hill slope for more than half a century.

To ensure the safety of Hong-Yeh Village and the functionality of countermeasures, results from this study were used to assess the likelihood of landslide recurrence and the feasibility of control structures. Modifications on countermeasure structures were made accordingly and promptly based upon data analysis from inclinometer readings, water-level readings as well as numerical simulations under several storm return period scenarios.

2. METHODS

2.1 Field geological survey

The purpose of field geological survey was to log the locations of outcrop, cleavage, stratification, joint, and the corresponding attitude. Geological phenomena such as existence of shear zone and tension cracks as well as signs of slope instability; such as unusual seepage, road slump, and cracks in structures that helped identify the possible causes or bearings of sliding were also documented.

2.2 Core drills and rock mechanical analyses

Total of five boreholes along the landslide scarp and right-side ridge was drilled on Apr. 12, 2017. Depths of drill varied from 20 m to 59 m.

Core samples from each borehole were taken for mechanical property analysis, which included Uniaxial Compression and Direct Shear Strength Tests on rock samples, Direct Shear Strength, Triaxial Consolidated Drained cohesion, Hydraulic Conductivity Tests on remolded soil samples.

2.3 Electrical Resistivity Image Profiling

Electrical Resistivity Image Profiling (RIP) was conducted by deploying two routes perpendicular to strikes of slate. Route 1 (RS1) ran between borehole #1 (B1) and borehole #2 (B2) with the stretch of 385 m; whereas, Route 2 (RS2) ran across borehole #4 (B4) with the stretch of 275 m.

2.4 In situ monitoring

Dual-axis inclinometer was used to take monthly displacement readings from ground level to the bottom of each borehole. Rain gauge was installed in the vicinity of the landslide site with a data logger attached to record rainfall events automatically. Water-level sensor was placed in each borehole casting to log groundwater levels continuously at 10-minute interval. It was then retrieved for data readout every month or shorter duration when needed.

2.5 Construction of digital elevation models

Digital elevation models (DEMs) were created using land survey resources gathered by different government agencies from different periods, which included Taitung County 1:1000 DEM taken in 2010, high-resolution Light Detection And Ranging (LiDAR) scan taken in 2012, 1-m DEM generated from aerial photos taken in 2014 by Forestry Bureau Aerial Survey Office, and 1-m DEMs generated from Unmanned Aerial Systems (UAS) images taken on Feb. 18, 2017 after emergency relief and June 19, 2017 during the construction of gully controls.

2.6 Numerical simulation of debris-flow affecting areas

FLO-2D model [*O'Brien et al*, 1993; *O'Brien*, 2003] was used to simulate the possible extent of debris-flow affecting areas under 50- and 200-yr storm recurrence intervals. Log-Pearson Type III Distribution was used for hydrologic frequency analyses to get one-day maximum rainfall, and Digital Elevation Models as previously described were used as terrain baseline maps respectively for periods prior to the disaster and during gully control constructions.

DEM with design elevations reflecting the final elevations at the completion of gully controls were also used to predict the likely debris-flow affecting areas as well as to identify the locations of overflow. Simulation results thus generated were used during gully control constructions for design adjustment or improvement. Standards for Debris-flow hazard zoning proposed by Rickenmann [2001], which considered flow velocity and maximum flow depth of the debris-flow, was used in this study to delineate levels of risk induced by debris-flow.

3. RESULTS AND DISCUSSION

3.1 Geology and micro-terrain interpretation

Results from field geological survey indicated that attitude of cleavage at landslide site was N12°W~N16°E, dip angle was 21°SE~30°NE, and the representative apparent dip was about 26°; whereas, attitude of cleavage and dip angle at the landslide scarp was N24°~36°E and 22°~34° SE respectively.

Field survey also found the representative weak planes formed by J1 and J2 joint (**Fig. 2**) respectively that affecting hillslope stability. J1 joint is less apparent and discontinuous; whereas, J2 joint forms the major joint with good ductility that fractures the rock stratum for more than 1 m and quartz veins [*Yang*, 2010] was found along tension joint fissures. Evidence collected onsite suggested that J2 joint was the weak plane that mainly affected the hillslope stability and caused landslide to occur.

Micro-terrain interpretation was conducted by analyzing satellite images and orthophotos taken from various periods. Interpretation results suggested that hillslope behind Hong-Yeh Village not only possesses avalanche features but also experienced large-scale landslide during modern geological history. **Fig. 3** is the results obtained from micro-terrain interpretation, in which boundaries of suspected potential slump mass and that of landslide scarps were marked.

By comparing the satellite images taken in 2016 and orthophotos taken on Feb. 18, 2017, a 240-m long scarp was also detected. Second field survey was carried out and the distribution of black-gray slate and highly weathered yellow sandstone was found at the detected scarp. Location of massive slump that matched the location where small-scale slump took place in 2012 was also discovered.

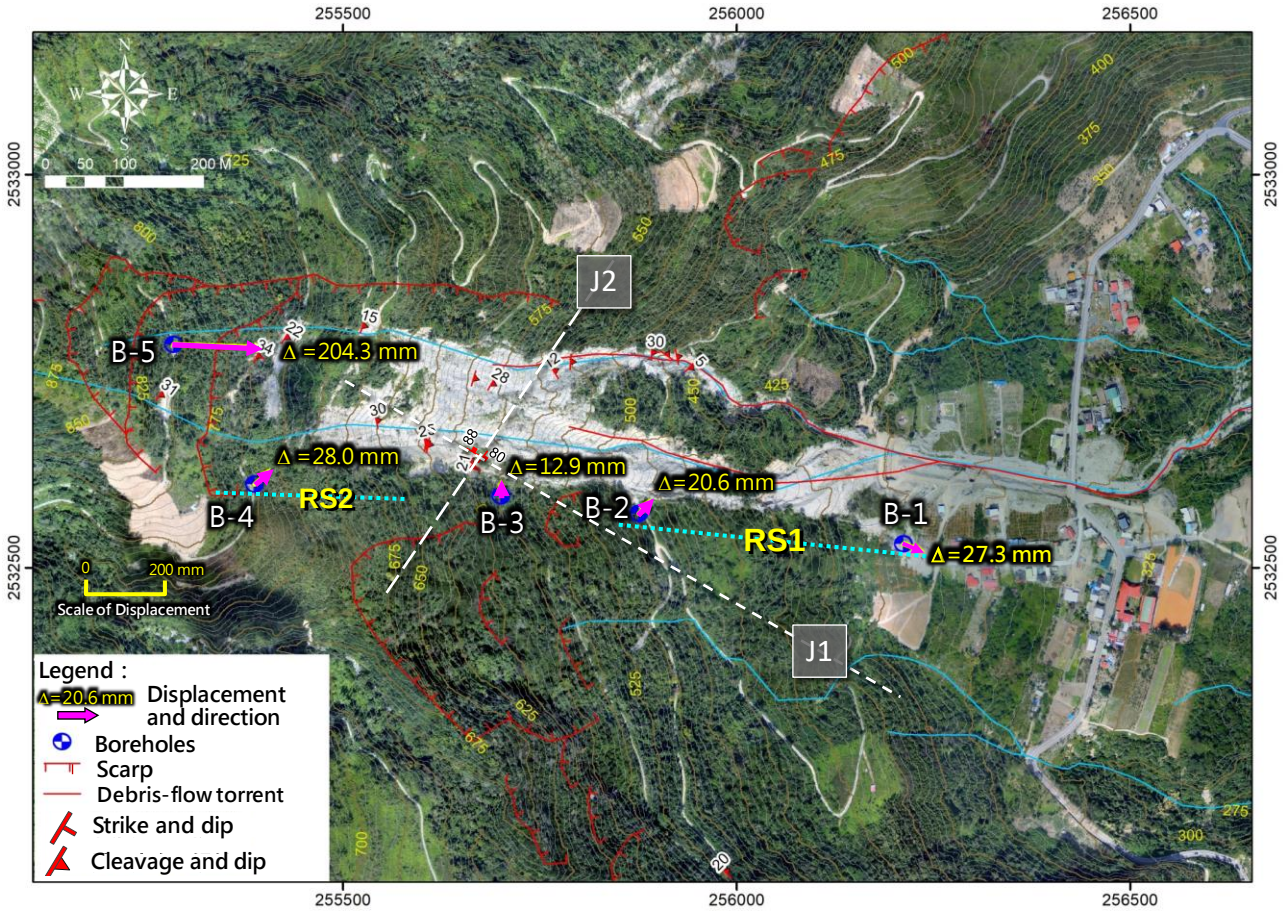

Fig. 2 Results of field geological survey and total displacement readings from each borehole

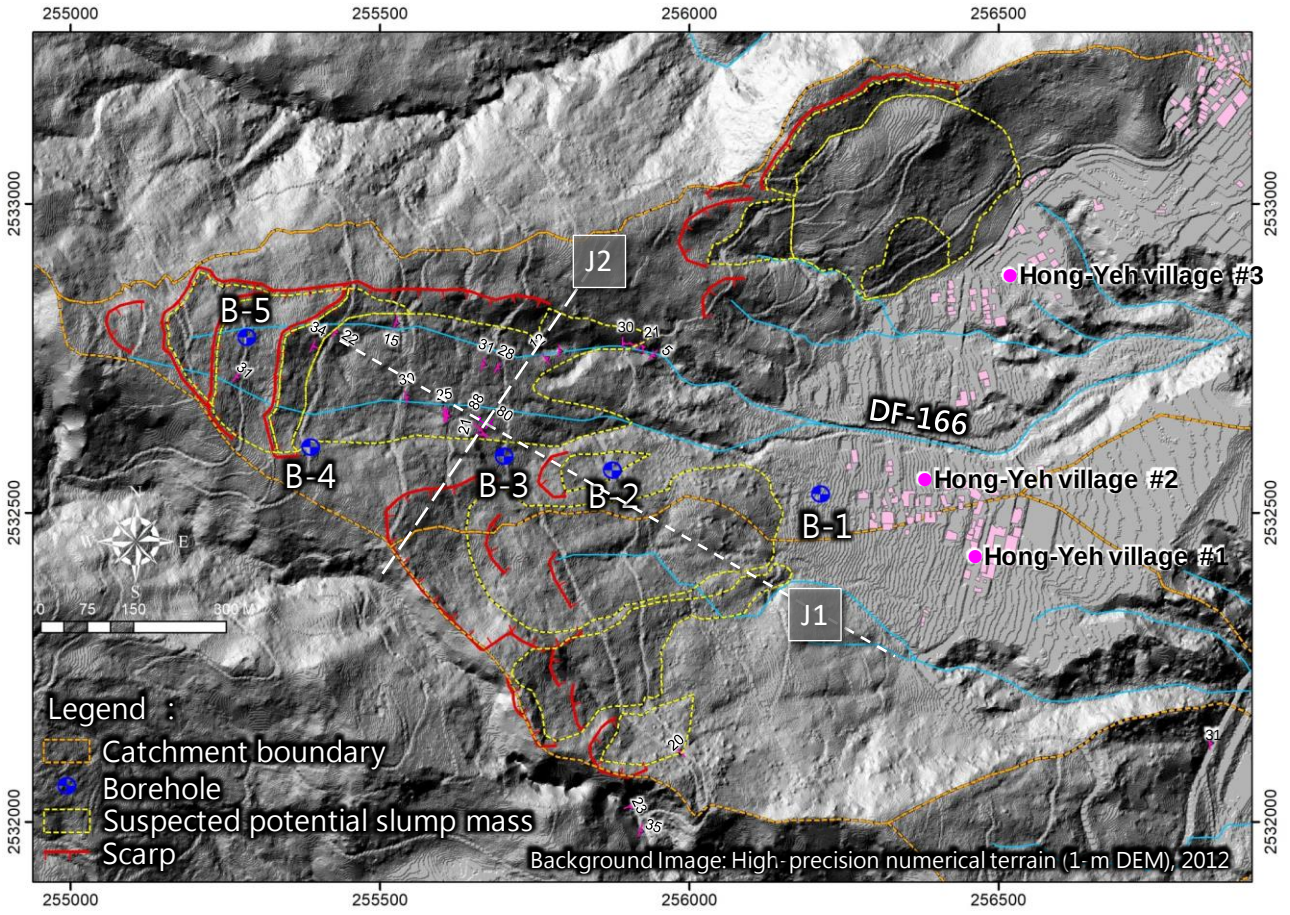

Fig. 3 Results of micro-terrain interpretation

3.2 Borehole samples interpretations and Electrical Resistivity Image Profiling results

By examining the depths of colluvial deposits from five boreholes′ core samples and the field findings from fresh outcrop survey, we were able to estimate the thickness of colluvial deposits as that shown in **Fig. 4**.

Estimation of colluvial deposits especially the extent of unstable mass as that shown in **Fig. 4** helped corresponding government agencies as well as residents of Hong-Yeh Village prepare for the worst scenario to come. It also helped emergency relief task forces to seek all control practices options and landslide recovery actions.

Electrical resistivity distribution readings taken along Route 1 (RS1) and Route 2 (RS2) suggested that rock stratum at the landslide site consists of three main layers. They are colluvial deposits, fracture zone, slate, and/or slate and sandstone interbed, where are denoted as ①, ②, and ③ respectively in **Fig. 5**.

Colluvial deposits covers from ground level to 50 m below, which were resulted from mass movements occurred at different periods. Core samples taken from borehole B-1 also confirmed the existence of colluvial deposits.

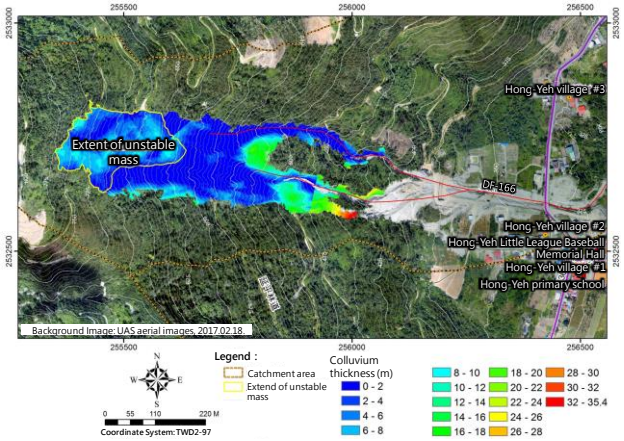

Fig. 4 Estimated thickness of colluvial deposits

Joints are abundant in the fracture zone so that surface water can easily seep into and form water pockets that were clearly registered in electrical resistivity readings as that shown in **Fig. 5**. This fracture zone may affect the stability of hillslope and the maximum affecting depth may reach 50 m.

3.3 Inclination and water-level monitoring

Total displacement (Δ) with respect to borehole bottom within 5-month period (from 2017/04/22 to 2017/09/27) was marked for each borehole along

with the displacement vector as that shown in **Fig. 2**.

The monthly average displacement rate taken from borehole B-1 to B-4 was 5.5, 4.1, 2.6, and 5.6 mm/mo. respectively; whereas the monthly average displacement rate from B-5 reached 40.9 mm/mo., which met the confirmed mass movement criterion proposed by Japan Association for Slope Disaster Management [2007].

The active moving zone in B-5 that estimated from inclination readings in the A-axis direction (pointing downslope) was about 21.0 ~ 21.5 m underneath the ground surface as that shown in **Fig. 6**. Inclination readings from B-5 also indicated that landslide is continuously moving in a rapid speed. All these evidences clearly verify the existence of dip slope.

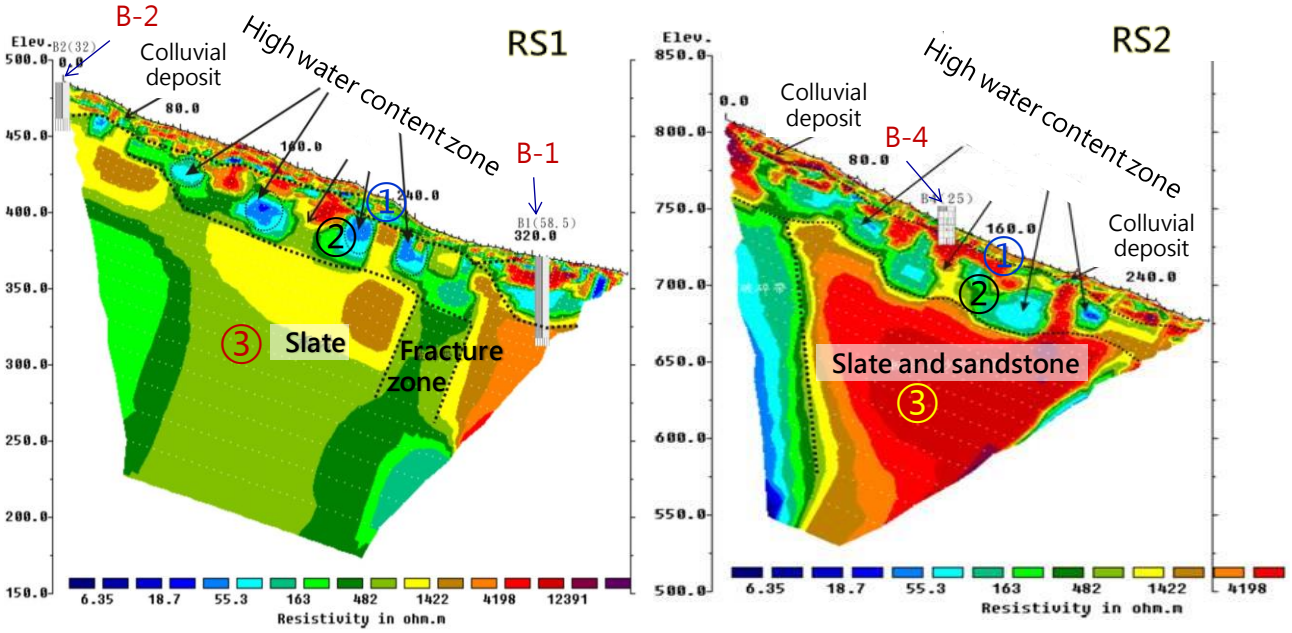

Fig. 5 Electric resistivity readings from Route 1 (RS1) and Route 2 (RS2)

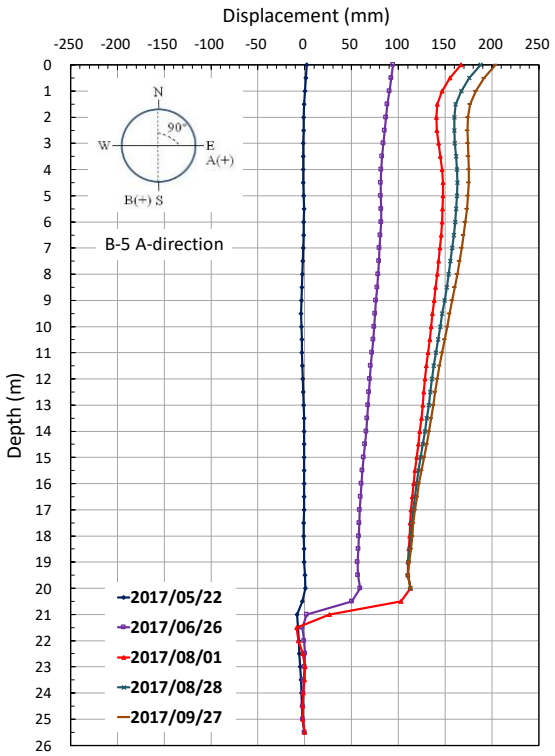

Fig. 6 Inclination readings from borehole B-5

Monitoring water levels in boreholes began in April 2017. **Figs. 7**, **8**, and **9** showed the records of water level elevations obtained from B-2, B-3, and B-5 respectively. 'Colluvial Deposits', 'Slate', and 'Fracture Slate / Sandstone' that marked in **Figs. 7**, **8**, and **9** was based on the readings from corresponding borehole core samples. Because of continuous sliding of the active moving stratum where B-5 was located, water-level sensor deployed in B-5 was unable to retrieve for data download after Oct. 8, 2017 9:50 a.m. Therefore, B-5 water level monitoring was forced to terminate.

In general, water levels in borehole were found synchronized with rainfall for B-2, B-3, and B-5 that situated along the landslide scarp. In contrast, there were almost no apparent changes in water levels for B-1 and B-4.

Three rainfall events occurred on June 3, July 4, and July 30 which brought 117.5, 91.5, and 204.5 mm of rain with the maximum hourly intensity of 16.5, 71.0, and 29.0 mm/hr to the site respectively. The water level in B-5 rose on June 3 and July 30 events to the elevation where suspected active moving stratum was located, but not on July 4 event as that

shown in **Fig. 9**. One of the possible reasons that causing no response of water level in B-5 on July 4 event was the sliding of active moving stratum (**Fig. 6**) that rearranged the stratum structure, porosity, and permeability. The entire hillslope at the vicinity of B-5 moved 50 ~ 100 mm between May 22 and June 26 and continued its movement with approximately the same speed that led to a total displacement of 204.3 mm at B-5 as that shown in **Fig. 2**.

In addition, a 5-day 924-mm torrential storm (10/11 Storm) from Oct.12 till Oct. 16 with peak one-day rainfall of 407 mm on Oct. 15 caused significant rise of water level at all boreholes except B-4. The maximum rise of water level was 0.8, 19.7, and 8.7 m for B-1, B-2, and B-3 respectively. The amount of rainfall brought by 10/11 Storm already exceeded 24-hour rainfall / 15-day cumulative rainfall prior to landslide occurrence criterion of triggering disastrous slope failure [*Lump*, 1962, 1975; *Brand*, 1982, 1989]. DEMs generated from UAS survey after 10/11 Storm confirmed the unstable mass situated in upper landslide site as that marked in **Fig. 4** moved 6.5 m eastward but slightly southward.

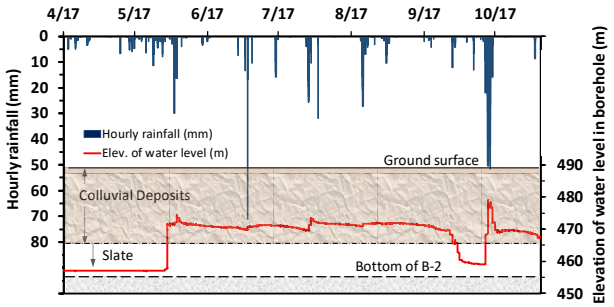

Fig. 7 Records of elevation of water level from borehole B-2

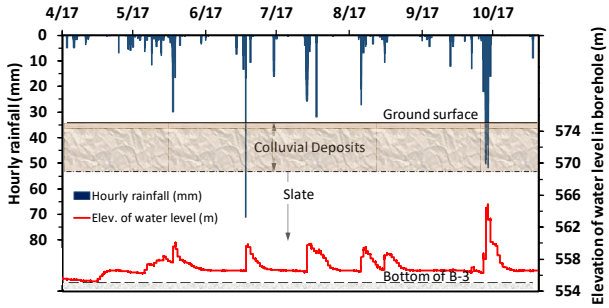

Fig. 8 Records of elevation of water level from borehole B-3

3.4 Landslide recurrence assessment

Judged by results from field geological survey, landslide scarp, micro-terrain interpretation, stratum distributions from core samples as well as inclinations and water level readings in boreholes, we reached the conclusion that recurrence of landslide is very likely. We speculate future landslide will probably occur in four levels as illustrated in **Fig. 10**. The total unstable mass counting all four levels was estimated to reach 920,000 m^3.

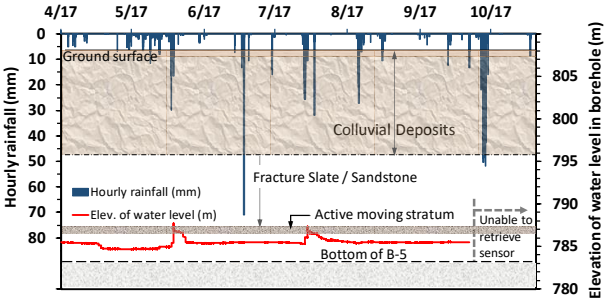

Fig. 9 Records of elevation of water level from borehole B-5

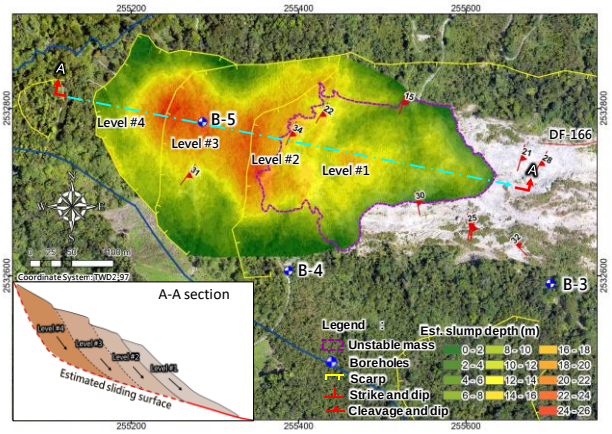

Fig. 10 Recurrence of possible sliding in levels

3.5 Debris-flow simulation

FLO-2D was used to estimate the extent of flooding and level of risk induced by debris flow. **Table 1** summarizes the results of numerical simulations at three event scenarios. All scenarios were conducted to simulate sediment-laden flow. The rheological parameters including fluid viscosity and yield stress as well as sediment concentration was carefully selected based upon the best judgement learned from debris flow residuals that observed from field survey performed on Sept. 16, 2016 immediately after the debris-flow disaster and recommendations proposed by FLO-2D.

Table 1 Levels of risk induced by debris flow

Scenario		Risk Classification			Total
		High	Med.	Low	
I	Area (m^2)	7,204	197	30,062	37,463
II	Area (m^2)	16,184	754	27,140	44,078
	% diff.	124.7	282.7	-9.7	17.7
III	Area (m^2)	3,286	145	19,014	22,445
	% diff.	-54.4	-26.4	-36.8	-40.1

Scenario I used the high-precision DEM map generated from the orthophotos taken on Aug. 15, 2014, which provided good topographic presentation of the landslide site prior to the landslide disaster. Runoff from 50-yr return period was used as inflow.

Scenario II used the high-precision DEM map generated by UAS taken on Feb. 18, 2017, which characterized the topography during the early stage of gully control constructions. Runoff from 50-yr return period was also used as inflow.

To cope with extreme event, sediment-laden runoff from 200-yr return period was used as inflow; whereas LiDAR survey when 50% of the control measures reaching to its completion was conducted to generate an updated DEM topographic base map for FLO-2D simulations. The extent of debris-flow risk caused by 200-yr return period is shown in **Fig. 11**.

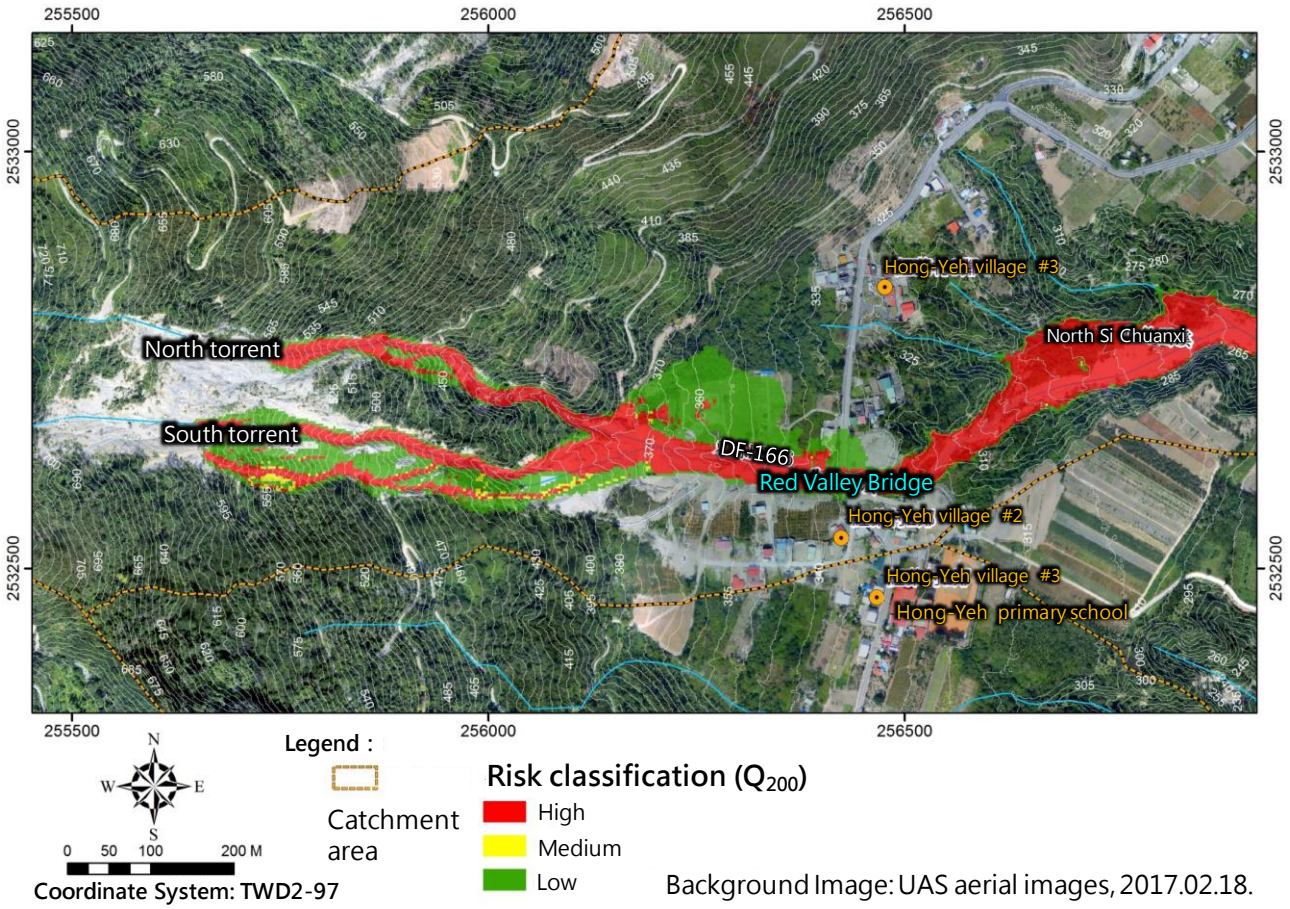

Fig. 11 Extent of debris-flow risk from 200-yr return period event if occurred during the construction of countermeasures

Simulation results shown in **Fig. 11** indicated that there was a weak spot along the left embankment after the confluence where North and South torrents met, at which 200-yr return period debris flow may overflow. Another possible overflow spot was likely to occur before Red-Valley Bridge because the clearance under Red-Valley Bridge was insufficient to convey the flood.

Scenario III simulation was carried out by altering the elevations at left embankment, clearance under Red-Valley Bridge, and channel cross section after Red-Valley Bridge. Runoff from 200-yr return period was also used as inflow.

Fig. 12 illustrated the simulation results using the topographic map obtained from field topographic survey conducted on June 19, 2017, which represented the completion of gully controls with necessary adjustments at spots where overflow or debris clogging may likely occur. Adjustment involved in gully control designs included increasing left embankment height by 2.5 ~ 3.0 m, increasing Red-Valley Bridge clearance to 7.0 m, and expanding channel width to 22.0 m. Results summarized in **Table 1** showed that 40.1% reduction in risk extent from 37,463 m^2 of Scenario I to 22,445 m^2 of Scenario III.

4. CONCLUSIONS

Heavy rainfall produced large amount of surface runoff that rushed into DF-166 high potential debris-

flow torrent and caused severe scour at the torrent bed. The sever scour at the torrent bed induced slope slump at both banks of the torrent. Early colluvial deposits with high permeability constitute most parts of the stratum so that rainwater could easily infiltrate into the deposits and cause reductions in shear resistance. The chain reaction consequently began. Continuous rainfall brought by Typhoon Aere, development of tension cracks along landslide scarp, and movement of unstable mass at the upper reach of landslide scarp further deteriorated the status of landslide.

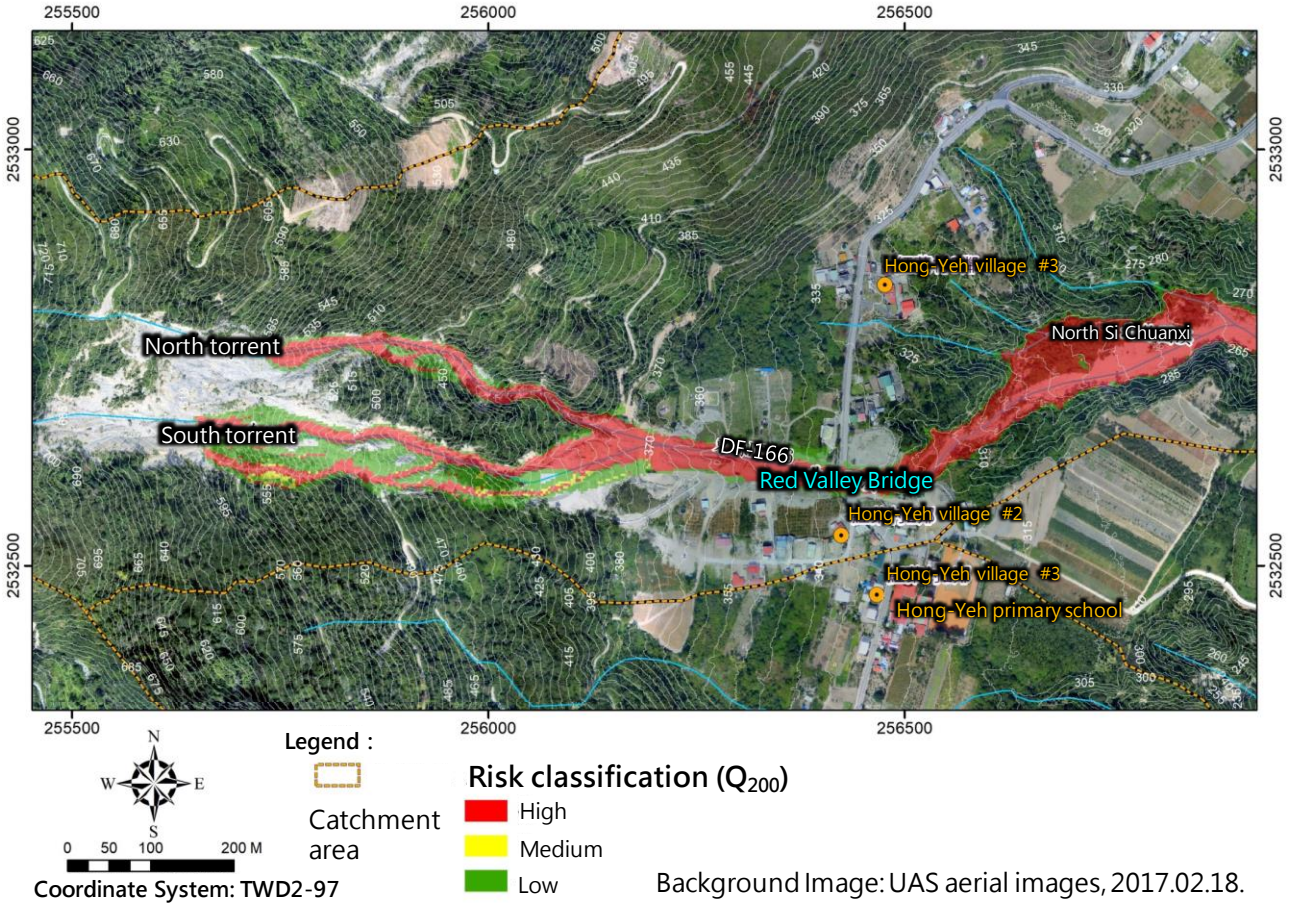

Fig. 12 Extent of debris-flow risk from 200-yr return period event if occurred after the construction of countermeasures

Construction of check dam and gully control structures reached completion in November 2017, which marked the end of the first phase of reconstruction project. Numerical simulations with three storm scenarios helped foresee the weak spots in control structure design.

Field geological survey, outcrop assessment, micro-terrain interpretation, core samples from borehole drill as well as inclination and water stage readings from five boreholes all suggests the cause of Sept. 15 landslide was mainly due to continuous, heavy rainfall and existing rock fractures. Hence, the likelihood of landslide recurrence is expected.

Recurrence of Hong-Yeh landslide is certain. However, there are still many issues that are uncertain including the scale, volume, and frequency of recurrent landslide, which require further investigations and onsite detail monitoring.

The second phase of reconstruction project is current on its way to detail design mainly on slope stabilization as well as continuous onsite monitoring the inclination, ground surface displacement along the landslide scarp and water-level changes in boreholes. An automatic monitoring system is scheduled for online operation at the site in mid-2018 so that rainfall amount, ground surface displacement, and water level stages can be monitored at remote office instantaneously.

ACKNOWLEDGMENT: Outcomes of this study were the join efforts from Lipang Engineering Consultant Co. Ltd., National Pingtung University of Science and Technology, Dept. of Soil and Water Conservation, Soil Erosion Research Unit, and Soil and Water Conservation Bureau Taitung Branch Office. The assessment project was funded under FY2017 SWCB-106-157 contract.

REFERENCES

Brand, E. W. (1982): Analysis and design in residual soils, Proceedings of the ASCE Geotechnical Engineering Division Speciality Conference on Engineering and Construction in tropical and residual soils, Honolulu, Hawaii, January 11-15.

Brand, E. W. (1989): Correlation between rainfall and landslides, Proceedings of the 12th International Conference on Soil Mechanics and Foundation Engineering, Vol. 5.

Japan Association for Slope Disaster Management (2007): Landslide Countermeasure Technical Design Implementation Manual (in Japanese).

Lumb, P. (1962): Effect of rainstorms on slope stability, Proceedings of the Symposium on Hong Kong soils, Hong Kong, pp. 73-87.

Lumb, P. (1975): Slope failures in Hong Kong, Quarterly Journal of Engineering Geology, Vol. 8, pp. 31-65.

O′Brien, J. S. (2003): FLO-2D User Manual, FLO-2D Software, Inc.

O′Brien, J.S., Julien, P.Y., and Fullerton, W. T. (1993): Two-dimensional water flood and mudflow simulation. Journal of Hydraulic Engineering, ASCE, Vol. 119, No. 2, pp. 245-261.

Rickenmann, D. (2001): Methoden zur Gefahrenbeurteilung von Murgangen. In: Projet CADANAV, Etablissement d'une methodologie de mise en oeuvre des cartes de dangers naturels du canton de Vaud; 2eme rapport intermediaire, Ecole Polytechnique Federal de Lausanne, Switzerland.

Yang, C.N. (2010): A case study on age relationship between obliquely intersected quartz veins in metasandstone, Taiwan Mining Industry, Vol. 62, No. 4, pp. 16-26 (in Chinese with English abstract).